Optical Characterization of Contrast Agents for Optical Coherence Tomography

Tin-Man Lee[1,3], Farah Jean-Jacques Toublan[2], Amy Oldenburg[1,3], Shoeb Sitafalwalla[3], Wei Luo[3], Daniel L. Marks[1,3], Kenneth S. Suslick[2], Stephen A. Boppart[1,3,4]

[1]Department of Electrical and Computer Engineering
[2]School of Chemical Sciences
[3]Beckman Institute for Advanced Science and Technology
[4]Bioengineering Program, College of Medicine
University of Illinois at Urbana-Champaign

ABSTRACT

The use of contrast agents in almost every imaging modality has been known to enhance the sensitivity of detection and improve diagnostic capabilities by site-specifically labeling tissues or cells of interest. The imaging capabilities of Optical Coherence Tomography (OCT) need to be improved in order to detect early neoplastic changes in medicine and tumor biology. We introduce and characterize the optical properties of several types of optical contrast agents in OCT, namely encapsulating microspheres that incorporate materials including melanin, gold, and carbon. Micron-sized microspheres have been fabricated by state-of-the-art sonicating and ultrasound technology. The optical properties of optical contrast agents have been characterized according to their scattering and absorption coefficients and lifetimes using OCT and the oblique incidence reflectometry method. Finally, we demonstrate the use of these optical contrast agents in *in vitro* mice liver and analyze the contrast improvement from the OCT images. These optical contrast agents have the potential to improve the detection of *in vivo* pathologies in the future.

Keywords: OCT, contrast agents, microspheres, scattering, absorption coefficients

1. INTRODUCTION

The use of these contrast agents in OCT has the potential to overcome the limitation of relying on inherent optical properties of the tissue to provide contrast to differentiate normal from pathological tissue. Increased OCT signals can be detected if more light is scattered back from regions of interest in tissues. This effect can be achieved by injecting highly scattering microspheres into tissue, or adhering the microspheres to specific tissue locations. Contrast enhancement by selectively locating contrast agents onto specific sites such as organs or tissues of interest has been successful in virtually every imaging methodology including ultrasound [1], computed tomography [2], magnetic resonance imaging [3], and fluorescent microscopy [4], to name a few. OCT is an emerging high-resolution diagnostic biomedical imaging modality [5-9]. Imaging in OCT, however, is frequently hindered by insufficient contrast difference between adjacent tissues. In order to identify early stage tumors in human tissues that are morphologically or optically similar to surrounding normal tissues, contrast enhancement on a specific site of interest is required. By targeting contrast agents to the cells or tissues of interest, the contrast gradient between different cells and tissues can be increased, rather than relying on the inherent optical properties of the tissue to provide contrast between normal and pathological tissues. The contrast agents in this study consisted of carbon, melanin and gold-coated encapsulating microspheres that are strong light scatterers. Thus, the tissues with injected contrast agents scatter more light and produce a stronger signal, leading to a contrast-enhanced OCT image. Previously, air-filled microbubbles have been used as contrast agents [10,11]. However, air-filled microbubbles

Genetically Engineered and Optical Probes for Biomedical Applications, Alexander P. Savitsky, Darryl J. Bornhop, Ramesh Raghavachari, Samuel I. Achilefu, Editors, Proceedings of SPIE Vol. 4967 (2003) © 2003 SPIE · 1605-7422/03/$15.00

suffer from short life-spans and cannot be engineered to scatter, absorb, or modulate light as is possible with the class of encapsulating contrast agents presented in this study. In addition, these encapsulating contrast agents can be targeted to specific sites by chemically modifying the surface of their shell.

2. CONTRAST AGENT PREPARATION

Contrast agents were prepared in several steps. First, high-intensity ultrasound was generated by a titanium horn with tip diameter of 0.5 inches driven at 20kHz. Second, a solution containing gold, melanin or carbon was prepared and added to a 5% weight per volume solution of bovine serum albumin (BSA). Third, high-intensity ultrasound was applied at the interface between the two solutions for sonication of the mixture. The size of the fabricated microspheres ranged from 0.5-15μm depending on the acoustic power and the frequency of ultrasound. By washing with nanopure water and filtering particle fragments and sizes, we selected microspheres that were 0.5-2μm in diameter. This size was selected to allow for passage through the microcirculation and as a size suitable for the cellular resolution of OCT imaging. The average size, size distribution, and concentration was measured using a Coulter Multisizer II Analyzer for each sample and for each type of contrast agent. To perform various optical characterization experiments, the contrast agent in solution was immobilized in a gel. Suspensions of microspheres in nanopure water were mixed with a solution of warmed liquid agarose and allowed to cool and solidify. The refractive index of the agarose gel was measured to be 1.34, which is similar to biological tissue.

Figure 1 shows a Scanning Electron Micrograph (SEM) of contrast agents with an oil-filled core and melanin incorporated into the shell. In this study, we characterized the optical properties of oil-filled microspheres with melanin, gold, and carbon nanoparticles incorporated into the shell. Control experiments were performed with protein-coated microspheres encapsulating oil. Encapsulating oil as a core material for these microspheres enabled these contrast agents to be more stable and robust compared to air-filled microbubbles. The average life-span for these oil-filled encapsulating microspheres typically ranged from 3 days to several months.

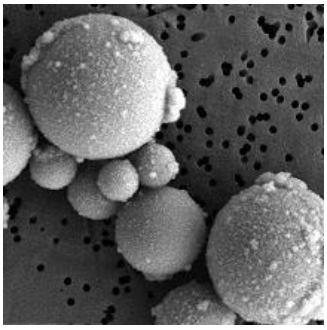

Figure 1: SEM image of the optical contrast agents.
(Image size 10μm x 10μm)

3. DATA COLLECTION

3.1. REFRACTIVE INDEX

The refractive indices of bulk melanin, gold, and carbon were obtained from the literature and are shown in Table 1. For comparison, samples of contrast agents mixed in agar were placed on the surface of a strong reflector and image-based measurements were made to determine the refractive index using a method previously described in the literature [12]. This method uses OCT to measure the physical and optical path lengths of the sample to determine

the average refractive index. The refractive indices of the encapsulating microspheres and the agarose gel were determined using this method. However in all cases, the measured average index of refraction was within the experimental error (5%) of the index of pure agarose. These similarities are likely due to the small fractional volume of the microspheres contained within the agarose gel.

3.2. REDUCED SCATTERING AND ABSORPTION COEFFICIENTS

The oblique-incidence reflectometry method incorporating a CCD camera and an 800nm laser diode was used to find the reduced scattering coefficient (μ_s') [13]. We chose this technique over an integrating sphere technique because it does not require a thin slice of tissue for both reflection and transmission measurements, and therefore can ultimately support *in situ* measurement of living tissues in conjunction with OCT imaging. From Table 1, it was determined that the reduced scattering coefficients of gold, melanin and carbon encapsulating microspheres are higher than oil alone, which demonstrate that these materials for our contrast agents can enhance local light scattering. Absorption coefficients were obtained from a Thermo Spectronic 20+ spectrometer by placing the contrast agent agar samples inside a curvette for analysis. The contrast agent and agar solution was dilute by a factor of 300 to facilitate measurements within the range of the spectrophotometer. Ten measurements for each contrast agent were obtained using wavelengths from 750 to 850nm. Transmission measurements were averaged and used to obtain the absorption coefficients from Lambert's Law,

$$T = 10^{-acx} \qquad [1]$$

where T = transmittance, a = absorption coefficient, c = molar concentration of the absorber, and x = thickness of curvette in centimeters. The results from the measurements at 800nm are shown in Table 1. As expected, the absorption coefficient for gold encapsulating microspheres is high, followed by that of the carbon and melanin encapsulating microspheres. All types were more absorbing that the protein-coated oil-filled control.

4. RESULTS

Table 1 summarizes the results of this study. The scattering and absorption cross-sections were determined based on the measured size distributions, the measured reduced scattering and absorption coefficients, and assuming an anisotropy factor (g) of 0.8.

Contrast agents	**Oil**	**Gold**	**Melanin**	**Carbon**
Size distribution (μm)	1.612 ± 0.722	1.853 ± 0.794	1.990 ± 0.985	1.660 ± 0.661
Refractive index	1.47 [14]	1.69 [15]	1.70 [16]	3.08 [17]
μ_s' cm^{-1}	10.80 ± 1.35	6.29 ± 0.76	18.29 ± 3.59	19.86 ± 4.33
μ_a (x10^{-4}) cm^{-1}	8.75	23.11	15.03	17.11
Scattering x-section (x10^{-6}) cm^2 per sphere	5.55	4.90	5.80	8.15
Absorption x-section (x10^{-10}) cm^2 per sphere	0.90	3.58	0.96	1.40

Table 1: Optical characterization of OCT contrast agents

5. IMAGING STUDIES

OCT images of Swiss mice (6 week old, 27 g, males) were obtained before and after contrast agents were injected. Mice were anesthetized by inhalation of halothane-soaked gauze prior to administration of contrast agents. A 1.3 μl solution of gold contrast agents was injected at a dose of 1.57 x 10^7 microspheres/μl via a tail vein. OCT was

performed before and 20 minutes after the injection. All animals used in this study were cared for and maintained under the established protocols of the Institutional Animal Care and Use Committee of the University of Illinois at Urbana-Champaign.

Our fiber-based OCT system consisted of a Nd:YVO_4 diode-pumped titanium:sapphire laser (Lexel Laser, Inc.) as a broad-bandwidth optical source which produced 500 mW average power and approximately 90 fs pulses with an 80 MHz repetition rate at 800 nm center wavelength. The output of this laser was coupled into an ultrahigh numerical aperture fiber (UHNA4, ThorLabs, Inc.) to spectrally broaden the light from 20 nm to over 100 nm, increasing the axial resolution of our system from 14 μm to 3 μm [18]. The UHNA4 fiber was spliced directly to the single mode fiber of a broadband 50:50 fiber coupler (Gould Fiber Optics, Inc.) which served as the beam splitter in a Michelson-type interferometer. The reference arm of the OCT interferometer contained a galvanometer-driven retroreflector delay line that was scanned a distance of 3 mm at a rate of 30 Hz to provide axial reflectance data. The sample arm consisted of a fiber-optic collimator to produce a 2 mm diameter beam from the fiber. The beam was focused into the tissue by a 12.5 mm diameter, 30 mm focal length achromatic lens to a 8 μm diameter spot size (transverse resolution). The beam was scanned over the tissue with a pair of orthogonal galvanometer-controlled mirrors. Approximately 6 mW of power was incident on the tissue. The reflected light was recollected by the lens and recombined in the fiber coupler with the delayed reference signal. The interference signal was measured by a silicon photodiode, bandpass-filtered by an analog filter, and rectified by a linear envelope detection circuit. The resulting scattering magnitude was digitized to 12-bit accuracy. Adjacent axial scans were assembled to produce two-dimensional OCT images that were displayed on the computer using custom data acquisition and display software.

Figures 2 and 3 show OCT images of mouse liver before and after the injection of gold encapsulating contrast agents, respectively. The liver was exposed for OCT imaging by shaving the abdomen, making a mid-line incision, and reflecting back the abdominal skin and peritoneal wall. The liver was imaged because this is one end-organ site for collection of these contrast agents as they are broken down and cleared from the circulation. The OCT image in Figure 2, acquired before the contrast agent was injected, shows little subsurface structure. A change in scattering is readily apparent in the image of Figure 3, following the intravenous injection of contrast agents. More structural detail is shown at greater depths in the contrast agent-enhanced liver image. We conclude that the contrast agents had accumulated in the microvascular network of the liver where they would be phagocytosed by Kupffer cells and broken down.

Figure 2: OCT image of mouse liver without contrast agent. Image size approximately 2 x 2 mm.

Figure 3: OCT image of mouse liver following injection of gold-encapsulating microsphere contrast agents. Note enhanced structural detail at greater depths. Image size approximately 2 x 2 mm.

6. CONCLUSION

We have developed, characterized, and demonstrated the use of encapsulating microspheres as contrast agents for OCT. Further investigations will include optimizing contrast agent enhancement by varying microsphere size and by encapsulating other scattering, absorbing, or modulating particles, and using other methods to verify our measurements, such as integrating sphere techniques. Similar to contrast agents in other imaging modalities, these contrast agents have the potential to increase the diagnostic utility of OCT by site-specifically targeting cells and tissues, particularly when pathological tissue is morphologically or optically similar to normal tissue.

7. ACKNOWLEDGEMENT

We wish to acknowledge the technical contributions of John Fahrner and thank The Whitaker Foundation (SAB), the National Institutes of Health (HL25934, KSS) and the Beckman Graduate Fellowship Program (TML) for their support of this research.

8. REFERENCES

1. C. Christiansen, H. Kryvi, P. C. Sontum T, Skotland, "Physical and biochemical characterization of Albunex, a new ultrasound contrast agent consisting of air-filled albumin microspheres suspended in a solution of human albumin", *Biotechnol. Appl. Biochem 19*, pp. 307-320, 1994.
2. G.S. Gazelle, G.L. Wolf, G.L. McIntire, E.R.Bacon, E.F.Halpern, E.R.Cooper, J.L.Toner, "Nanoparticulate computed tomography contrast agents for blood pool and liver-spleen imaging", *Acad. Radiol. 1*, pp. 373-376, 1994.
3. M.Y. Su, A. Muhler, X. Lao, O. Nalcioglu, "Tumor characterization with dynamic contrast-enhanced MRI using MR contrast agents of various molecular weights", *Magn. Reson. Med. 39*, pp. 259-269, 1998.
4. J.E. Bugaj, S. Achilefu, R.B. Dorshow, R. Rajagopalan, "Novel fluorescent contrast agents for optical imaging of in vivo tumors based on a receptor-targeted dye-peptide conjugate platform", *J. Biomed. Opt. 6*, pp. 122-133. 2001.
5. D. Huang, E. A. Swanson, C. P. Lin, J. S. Schuman, W. G. Stinson, W. Chang, M. R. Hee, T. Flotte, K. Gregory, C. A. Puliafito, J. G. Fujimoto, "Optical Coherence Tomography", *Science 254*, pp. 1178-1181, 1991.
6. S.A. Boppart, G.J. Tearney, B.E. Bouma, J.F. Southern, M.E. Brezinski, J.G. Fujimoto, "Noninvasive assessment of the developing *Xenopus* cardiovascular system using optical coherence tomography," *Proc. Natl. Acad. Sci. USA 94*, pp. 4256-4261, 1997.
7. G.J. Tearney, M.E. Brezinski, B.E. Bouma, S.A. Boppart, C. Pitris, J.F. Southern, J.G. Fujimoto, "*In vivo* endoscopic optical biopsy with optical coherence tomography", *Science 276*, pp. 2037-2039, 1997.
8. M.V. Sivak Jr, K. Kobayashi, J.A. Izatt, A.M. Rollins, R. Ung-Runyawee, A. Chak, R.C. Wong, G.A. Isenberg, J. Willis, "High-resolution endoscopic imaging of the gastrointestinal tract using optical coherence tomography", *Gastrointest. Endosc. 51*, pp. 474-479, 2000.
9. S. A. Boppart, B. E. Bouma, C. Pitris, J. F. Southern, M. E. Brezinski, J. G. Fujimoto, "In vivo cellular optical coherence tomography imaging", *Nature Medicine 4*, pp. 861-865, 1998.
10. M.W. Grinstaff, K.S. Suslick, "Proteinaceous microbubbles: synthesis of an echo contrast agent", *Proc. Natl. Acad. Sci. USA 88*, pp. 7708-7710, 1991.
11. J.K. Barton, J.B. Hoying, C.J. Sullivan, "Use of Microbubbles as an Optical Coherence Tomography Contrast Agent", *Academic Radiology 9S*, pp. 52-71, 2002.
12. Tearney G J, Brezinski M E, Southern J F, Bourna B E, Hee M R and Fujimoto J G, "Determination of the refractive index of highly scattering human tissue by optical coherence tomography", *Opt. Lett. 20*, pp. 2258-60, 1995.
13. L. Wang, S.L. Jacques, "Use of a laser beam with an oblique angle of incidence to measure the reduced scattering coefficient of a turbid medium", *Appl. Opt. 34*, pp. 2362-2366, 1995.

14. S. K. Kurtz, S. D. Kozikowski and L. J. Wolfram, “Nonlinear optical and electro-optical properties of biopolymers”, *Electro-optics and photorefractive materials (edited by P. Gunther)*, pp. 110-130, 1986.
15. Palik, ed., Handbook of Optical Constants of Solids I and II, 1991.
16. A. Vitkin, J. Woolsey, B. C. Wilson, R. R. Anderson, “Optical and thermal characterization of natural (sepia officinalis) melanin”, *Photochemistry and Photobiology 59*, pp. 455-462, 1994.
17. C. F. Bohren and D. R. Huffman, “Absorption and Scattering of Light by Small Particles”, 1983.
18. D.L. Marks, A.L. Oldenburg, J.J. Reynolds, S.A. Boppart, “Study of an ultrahigh-numerical-aperture fiber continuum generation source for optical coherence tomography”, *Opt. Lett* 27:2010-2012, 2002.